Journal of Structural Geology, Vol 13, No 7, pp 787 to 799, 1991
Printed in Great Britain

0191-8141/91 $03 00+0 00

Development of microcracks in granites during cooling and uplift: examples from the Variscan basement in NE Bavaria, Germany

AXEL VOLLBRECHT, SUSANNE RUST and KLAUS WEBER

Institut fur Geologie und Dynamik der Lithosphäre, Universität Göttingen, Goldschmidtstrasse 3, D-3400 Göttingen, Germany

(*Received* 20 *August* 1990; *accepted in revised form* 28 *January* 1991)

Abstract—Microcracks in two late-Variscan granites in NE Bavaria provide information about regional paleostress directions and *P–T* conditions during cooling and uplift. In both granites three prominent generations of healed microcracks (called CI, CII, CIII) constitute an orthorhombic fabric the orientation of which is closely related to the mesoscopic joint pattern.

We present a model relating this orthorhombic crack fabric not only to external deviatoric stresses, but also to internal stresses on the grain scale resulting from the strong thermal contraction of quartz relative to the feldspar framework.

At the deepest level (σ_1 subvertical), steep CI cracks developed normal to σ_3, and selectively in the quartz. Their formation caused a stress uncoupling of quartz aggregates from the external σ_3 direction, so that further contraction of quartz produced steep CII cracks normal to σ_2, forming bridges between CI cracks. At higher levels (σ_2 subvertical), the same process reactivated the CI cracks and now formed horizontal crack bridges (CIII). *P–T* estimates based on fluid inclusion data and inferred geothermal gradients are 250–400°C at 1.5–3 kbar for CI–CII cracks and 150–200°C at 1–2 kbar for CIII cracks. The orientation of the younger open cracks which formed at higher crustal levels partly corresponds to the present regional stress field.

INTRODUCTION

CRYSTALLINE rocks commonly display complex composite microcrack systems which have formed progressively by different geologic processes and under varying conditions (for a review on microcrack morphogenesis, kinematics and dynamics see Kranz 1983). Therefore detailed microcrack investigations can provide information on different stages of the (late) crustal evolution. For instance, paleostress directions may be inferred from preferred microcrack orientations (e.g. Pecher *et al.* 1985, Kowallis *et al.* 1987, Jang *et al.* 1989) and, in addition, for healed cracks the *P–T* conditions of formation can be estimated from microthermometry of the associated secondary fluid inclusions (e.g. Cathelineau *et al.* 1990).

Besides their geological significance, microcrack studies are of increasing interest in geophysics. Numerous recent studies have shown that the physical properties of rocks are not only controlled by the constituent minerals and their preferred orientation (for review see Kern & Wenk 1985) but also by the microcrack fabrics. This holds, in particular, for the anisotropy of elastic wave velocities (e.g. Thill *et al.* 1969, Siegesmund *et al.* 1991), electrical conductivity and permeability (e.g. Nover *et al.* 1989). Consequently, detailed knowledge about microcrack fabrics may also substantially improve the interpretation of geophysical field measurements and borehole loggings.

The present investigations were carried out as part of the Continental Deep Drilling Program of the Federal Republic of Germany (KTB), which is expected to reach a depth of at least 10 km within the Variscan basement of NE Bavaria. The major geoscientific objectives of the KTB are described in detail by Behr & Emmermann (1987) and Fuchs & Giese (1987). In this regard, microcrack analyses represent an interdisciplinary research program covering the above mentioned geological as well as geophysical topics. Another objective is to examine the influence of cracks on borehole and drillcore stabilities.

This paper deals with microcracks in two granites from the surrounding area of the KTB site. Based on crack fabrics, microstructural characteristics and fluid inclusion data, a comprehensive model of polyphase microcracking is developed which is closely related to the uplift history.

GEOLOGICAL SETTING

According to Kossmat (1927) the mid-European Variscides can be subdivided into several zones (Fig. 1a) showing distinct differences in sedimentary and tectonometamorphic facies. In terms of modern plate tectonics these zones are interpreted as terranes which were accreted to the southern margin of the Laurasia megacontinent (e.g. Ziegler 1984). The KTB study area is located in the Variscan basement of NE Bavaria (Oberpfalz, Germany) and is interpreted as part of the collision zone between the Moldanubian terrane to the southeast and the Saxothuringian terrane to the northwest (Fig. 1b). Extensive deep seismic reflection investigations support the model of SE-dipping master décollements along which Saxothuringian crust has been subducted under Moldanubian (e.g. DEKORP Research Group 1988, Vollbrecht *et al.* 1989; for overview on the extended geological framework see Franke 1989).

The structural development as deduced from surface

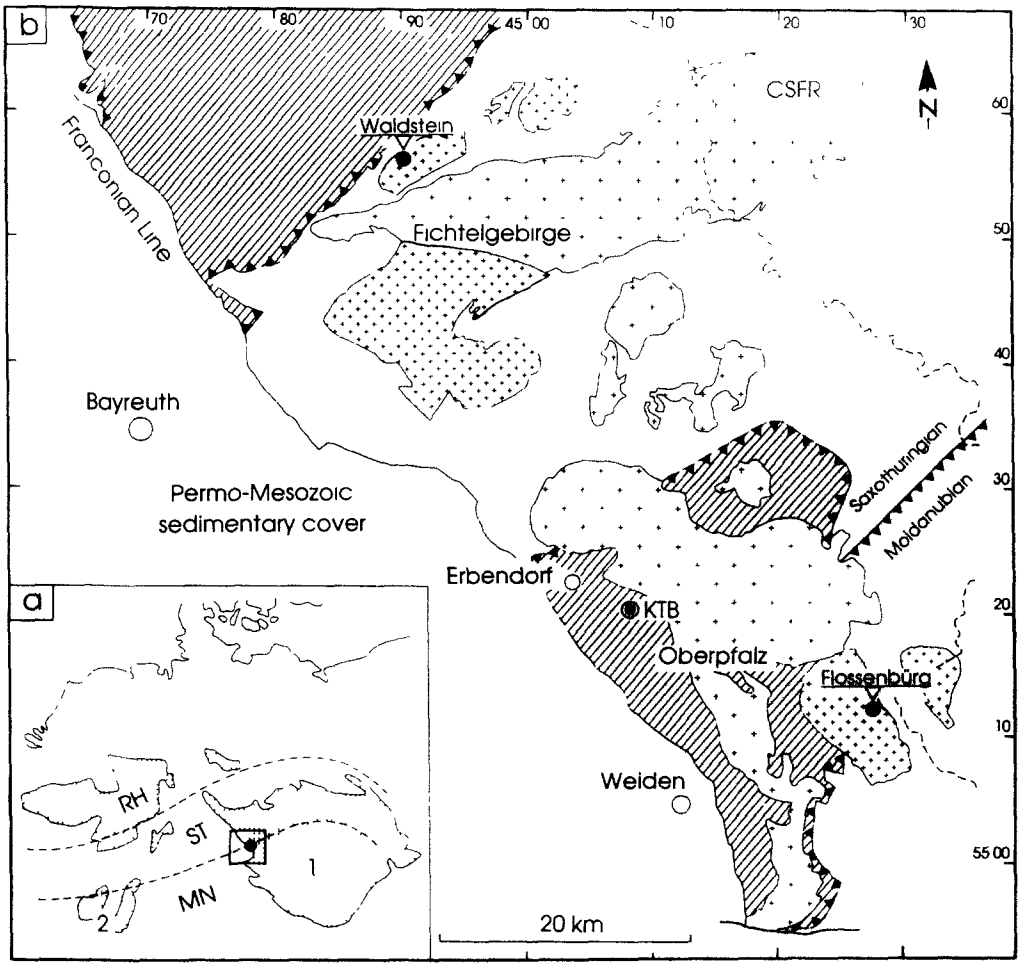

Fig 1. Geological sketch maps (a) Mid-European Variscan Zones after Kossmat (1927); RH—Rhenohercynian, ST—Saxothuringian, MN—Moldanubian; MN–ST boundary is exposed in the Bohemian Massif (1) and the Black Forest–Vosges area (2), inset outlines area of investigation as shown in (b) (b) Moldanubian–Saxothuringian collision zone in the Fichtelgebirge–Oberpfalz area (NE Bavaria, Germany) with the sample sites in the Waldstein and Flossenbürg granites and the KTB drilling location. Two groups of granites according to their K–Ar ages: 290–300 Ma (narrow-spaced crosses), 300–320 Ma (wide-spaced crosses); hatched: nappe piles containing units of medium- to high-pressure metamorphism

geology is characterized by polyphase folding and related thrust tectonics leading to complex imbrication patterns (Stein 1987, Weber & Vollbrecht 1989). Structures of the early collisional stage point to NW-directed transport and SE-directed backthrusting, whereas the late collisional stage is documented by SW-facing structures and subsequent NW-striking dextral wrench faulting. According to Weber (1986) the corresponding reorientation of the regional stress field can be interpreted in terms of a late N-directed arc-shaped indentation affecting the Southern German block between the Bohemian Massif and the Black Forest–Vosges area (Fig. 1).

During the early collisional stage the Moldanubian–Saxothuringian unit was affected by a high-temperature–low-pressure (HT–LP) metamorphism increasing continuously in grade towards the southeast and reaching conditions of anatexis at the northern margin of the Moldanubian (Schreyer 1966, Wagener-Lohse & Blümel 1984). Numerous geochronologic data consistently indicate ages of about 320 Ma for the peak of metamorphism (e.g. Teufel 1988, Hansen *et al.* 1989).

The uppermost structural level is represented by klippen of a nappe pile which, in contrast to the underlying Moldanubian–Saxothuringian unit, are characterized by a medium- to high-pressure metamorphism at about 380 Ma (e.g. Schüssler *et al.* 1986, Teufel 1988, Kreuzer *et al.* 1989), which is related to an earlier oceanic subduction stage (e.g. Weber & Vollbrecht 1989).

After the emplacement of these nappes and immediately after the peak of the HT–LP metamorphism the whole Moldanubian–Saxothuringian transition zone was intruded by late- to post-tectonic granites with ages ranging between 320 and 290 Ma (e.g. Köhler *et al.* 1974, Köhler & Müller-Sohnius 1976, Wendt *et al.* 1986). The samples selected for this study are from the Waldstein granite at the northern flank of the Fichtelgebirge anticline, and from the Flossenbürg granite at the northern margin of the Moldanubian, both belonging to the younger generation with ages of about 300–290 Ma (Fig. 1b).

The Franconian Line representing the main fault between basement and Permo-Mesozoic sedimentary cover is characterized by complex polyphase displacements during post-Variscan time with apparent vertical offsets up to about 2000 m.

SAMPLES

For detailed microcrack analyses two oriented samples from the Waldstein and one from the Flossenbürg granite were collected (Fig. 1b). In addition, seven further specimens from Waldstein and two from Flossenbürg were taken for petrographic examination and to check qualitatively whether the measured microcrack patterns display consistent orientations over the whole outcrop areas.

The macroscopic fabric of both granites is characterized by a medium- to coarse-grained matrix containing larger (up to 30 mm) aggregates or hypidiomorphic to idiomorphic grains of K-feldspar; macroscopically visible foliations or lineations are not developed.

According to Richter & Stettner (1979) the modal composition of the Waldstein granites is (in vol%): 37.5 quartz, 29.7 K-feldspar, 21.6 plagioclase, 6.6 biotite, 4.5 muscovite and 0.1 accessories. For the Flossenbürg granite the following vol% were recalculated from wt%-data given by Fischer (1965): 40.5 quartz, 20.6 K-feldspar, 26.9 plagioclase, 2.1 biotite, 8.1 muscovite and 1.8 accessories.

Microstructures and alteration phenomena are quite similar for both granites. K-feldspar occurs as microcline perthite or banded perthite, partly displaying a multiple primary zoning. Most of the plagioclase grains show polysynthetic albite twins which are interpreted as growth twins since microstructural features suggesting mechanical twinning are lacking. Both K-feldspar and plagioclase are affected by hydrothermal alteration (mainly sericitization) with varying intensities related to individual grains or their internal zoning. The quartz polycrystals display irregular lobate grain boundaries and undulose extinction. Only very few grains show deformation bands or lamellae. The mica flakes appear to be almost undeformed, only in some grains bending or kinking is observed, preferentially in small zones close to grain boundaries. Biotite is altered locally to chlorite. For further petrographic details see Fischer (1965) and Richter & Stettner (1979), respectively.

METHODS

Optical microscopy and U-stage measurements

For optical microscopy and U-stage measurements 25–30 μm thick standard thin sections were used. There is no evidence that a significant number of open cracks were produced during sample preparation, since they show a constant orientation in different thin sections and there is no relation between crack densities and sample geometry. Moreover, Fe oxide coating along open cracks indicates that they formed in a natural environment.

The U-stage measurements were carried out in three mutually perpendicular oriented thin sections in order to record all possible microcrack orientations. Composite pole figures were plotted for the horizontal plane (Schmidt net, lower hemisphere) using the computer program ARiAne (Adam 1989). Elevated crack pole densities resulting from the overlap of Schmidt net sectors of the three sections (for brief discussion see Siddans 1976) were statistically compensated by doubling the number of crack poles for areas of no overlap. Three-fold overlap was avoided by limiting the tilt angle at the U-stage to approximately 35° (Fig. 2). Disregarding this problem might result in spurious maxima and high-symmetric patterns, especially for samples with only weak or no (real) preferred crack orientations (e.g. Peng & Johnson 1972).

In order to examine whether microcracks show preferred crystallographic orientations, the *c*-axes of the host grains (quartz) were measured so that the angles between *c*-axes and cracks could be calculated. The corresponding frequency plots were reduced by the theoretical frequency distribution for random crack orientations with respect to a crystallographic axis, as calculated by Bloss (1957) (see Fig. 3).

Moreover, on account of the varied objectives of microcrack studies in the KTB for each individual crack, a comprehensive microstructural characterization was carried out considering features like crack dimensions,

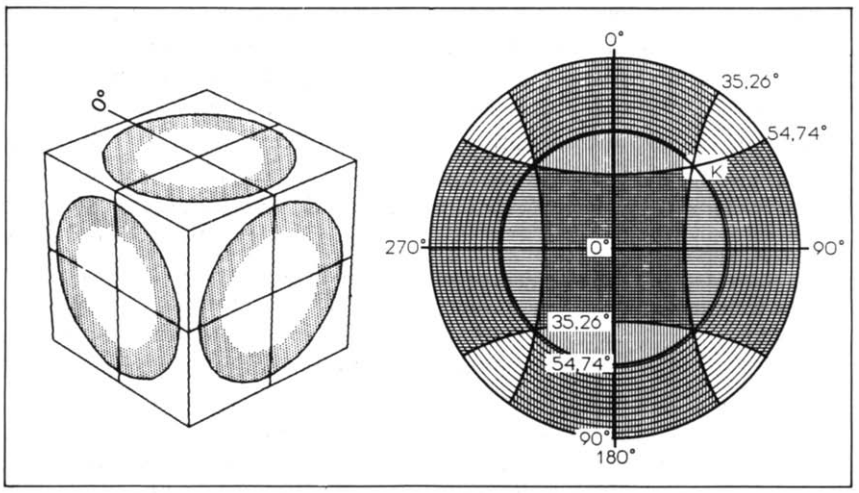

Fig. 2. Crack measurement in three orthogonal sections; sample cube and schematical crack pole plots. Crack poles are restricted to a marginal girdle due to limited tilt angles during U-stage measurements. Composite pole figure with areas of two-fold overlapping (cross-hatched) and areas of no overlapping (hatched); for further explanation see text.

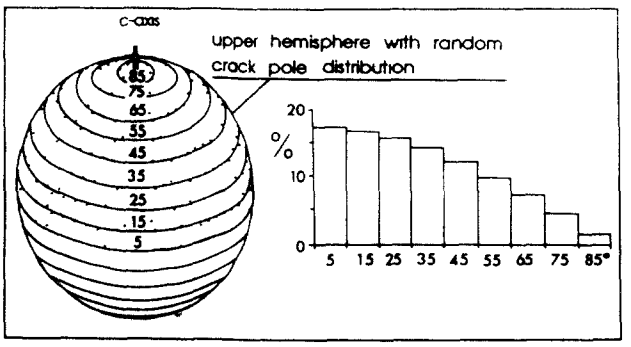

Fig 3 Crack poles with random orientation shown on the upper hemisphere and corresponding theoretical frequency plot of angles between crack pole and the pole axis (in this case representing the crystallographic *c*-axis), after Bloss (1957)

shape, state (open, healed, sealed), and geometrical relationships to other microstructures (e.g. grain and subgrain boundaries, cleavages, twins, deformation lamellae).

Microthermometry of fluid inclusions

For a microthermometric study of secondary fluid inclusions within healed microcracks a heating–freezing stage of the type Chaixmeca was used (Poty *et al.* 1976) and temperatures of eutectic melting (T_e), final melting (T_m) and homogenization (T_h) were measured following the instructions by Roedder (1984). To achieve a close correlation between orientation and fluid inclusion data the polished thick sections (90–110 μm; for sample preparation see Shepherd *et al.* 1985) were cut from the sample slices remaining from the corresponding thin sections. For the measurements, oriented fragments of the thick sections were placed on the heating–freezing stage and a detailed sketch of each fragment was made to enable later identification and reorientation with respect to a photograph of the complete section.

Inclusion densities (isochores) have been calculated from T_m and T_h data ignoring inclusions suspected of leakage or necking down. Leakage has been assumed, for example, where single inclusions showed strongly deviating T_m values compared with the majority of the other inclusions of the same trail. Necking down has been inferred from a general large scatter of T_h values within a single trail lacking any significant concentrations.

RESULTS

Microcrack fabrics

The most striking microstructural features observed in samples from both localities can be described as follows

(1) The overall crack pattern is dominated by healed cracks preferentially developed in quartz. Most of them are intragranular, frequently starting at grain boundaries. The crack density often changes drastically from grain to grain but shows no relation to the degree of plastic deformation of the host grains

(2) The corresponding secondary fluid inclusions are usually of the two-phase type (liquid–vapour, Fig. 4a) but leakage phenomena are frequent sometimes affecting the whole inclusion plane (Fig. 4b).

(3) These reopened former healed cracks often extend into open cracks or are aligned parallel to them.

(4) In particular healed cracks tend to form an orthorhombic pattern of two sets within individual quartz grains: a first generation of long cracks and a related subordinate second generation of shorter cracks. Cracks of the second set usually are terminated by cracks of the first set or form bridges between them (Fig. 4c).

(5) Compared with healed cracks, open cracks display more irregular shapes and larger dimensions often transecting several grain boundaries and phase boundaries (Fig. 4d).

(6) Completely sealed cracks are rare and only observed with sericite filling where healed cracks in quartz cross over into feldspar. Sections of open cracks are frequently coated by Fe oxides.

(7) All crack types appear to be tensile (mode I) since any microstructural evidence of lateral displacement is lacking.

In the Flossenbürg sample the cracks show significant preferred crystallographic orientations within the quartz host grains with a clear differentiation between open and healed cracks (Fig. 5). According to the frequency plot of angles between cracks and quartz-*c*-axes, healed cracks show a strong tendency to develop at low angles to the *c*-axis whereas the angles for open cracks scatter around 40°. This probably indicates that open and healed cracks formed by different mechanisms. One explanation is to relate the open cracks to rhombohedral cleavage planes while the orientation of healed cracks may be controlled by the direction of maximum thermal expansion which is normal to the *c*-axis (Skinner 1966). In addition, several microstructural features which are schematically illustrated in Fig. 6 also suggest that the direction of crack propagation is lattice-controlled

All generations of healed cracks show strong preferred orientations which obviously are coincident with the directions of macroscopic joints (Figs. 7a–d). According to previous studies (e.g. Hofmann 1957) this joint pattern is roughly the same in all granites of the Fichtelgebirge. The positions of maxima in the crack pole figures are essentially the same for both localities. Comparison with the other specimens qualitatively confirms that these crack patterns are fairly consistent over the whole outcrop areas. Healed cracks display an orthorhombic pattern composed of three sets: two steep sets striking NW and NE, respectively, the latter less pronounced, and one subhorizontal set (Figs. 7c–f). In agreement with microstructural observations (Fig. 4c) the pole maxima of the healed steep cracks show that short cracks (<150 μm) preferentially striking NW predominate (Figs. 7e & f)

In contrast to the healed cracks, the open cracks

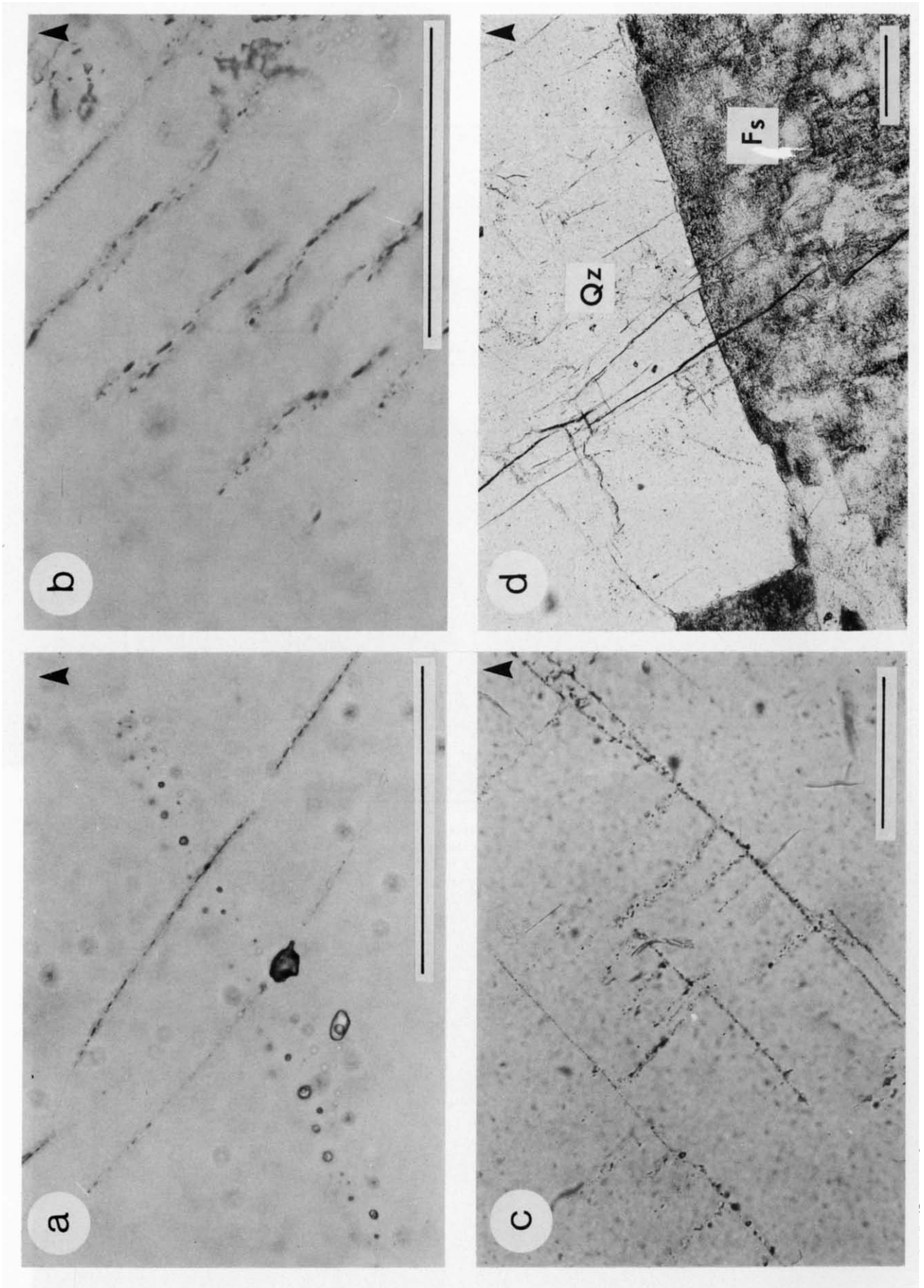

Fig. 4. Microstructural characteristics of microcracks in the investigated granites, oriented horizontal sections, N direction is indicated by arrows; scale bars = 0.1 mm. (a) Healed cracks in quartz outlined by planes of secondary fluid inclusions, two-phase type (liquid and vapour bubble); leakage in areas where fluid inclusions are cut by younger cracks (large dark inclusion in the center), Flossenburg (b) Planes of healed cracks in quartz with almost completely leaked secondary fluid inclusions; Waldstein (c) Orthogonal system of two sets of healed cracks in quartz; first generation of long NE-striking cracks connected by short bridges of the second generation; Waldstein (d) Long irregular open crack cutting quartz–feldspar (qz–fs) boundary; Flossenburg

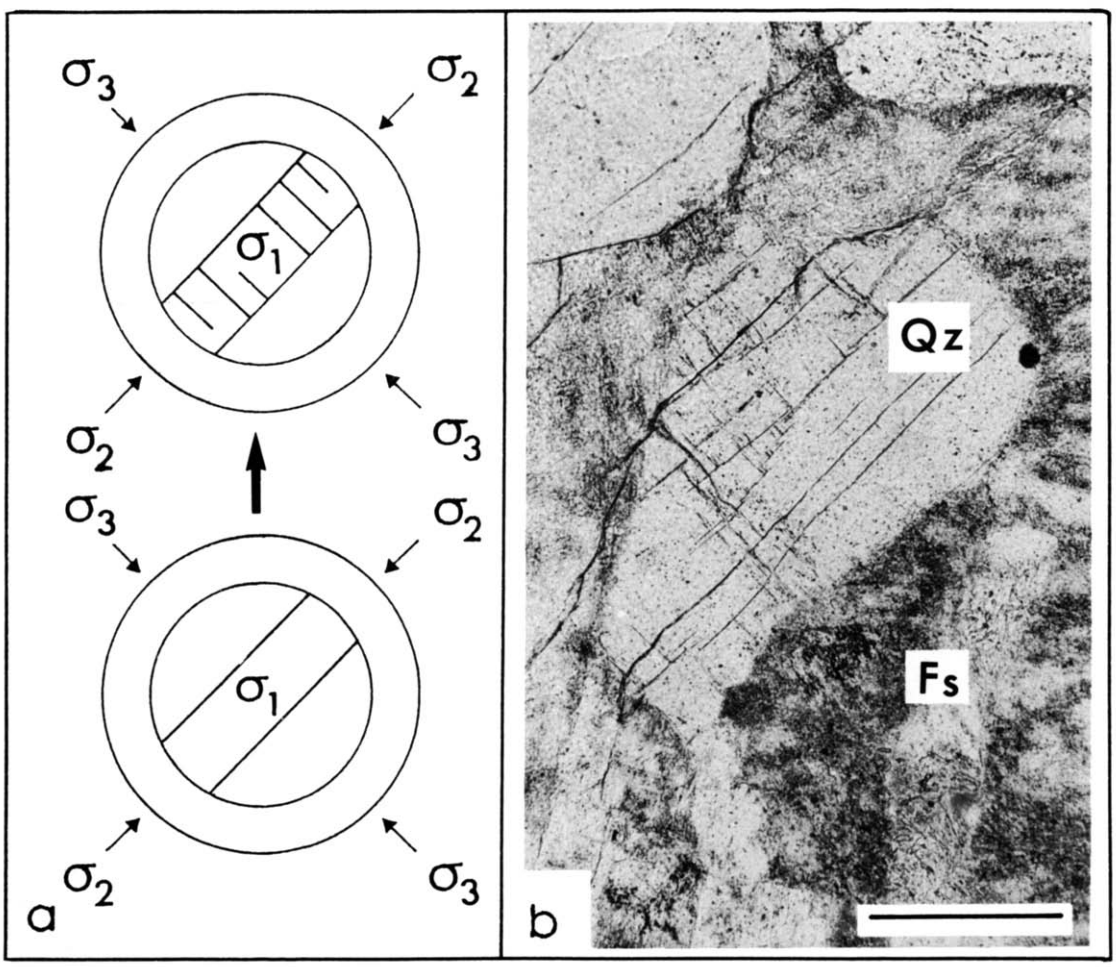

Fig 10 (a) Development of orthogonal crack pattern due to superposition of thermal stresses and external deviatoric stresses, for further explanation see text (b) Quartz inclusion in feldspar illustrating the main microstructural features indicative of thermal cracking during cooling as shown in (a) and Fig 9· higher crack density in quartz as compared with the surrounding feldspar, and two orthogonal sets of cracks (second generation of short cracks forming bridges between long cracks of the first generation); scale bar = 0.25 mm

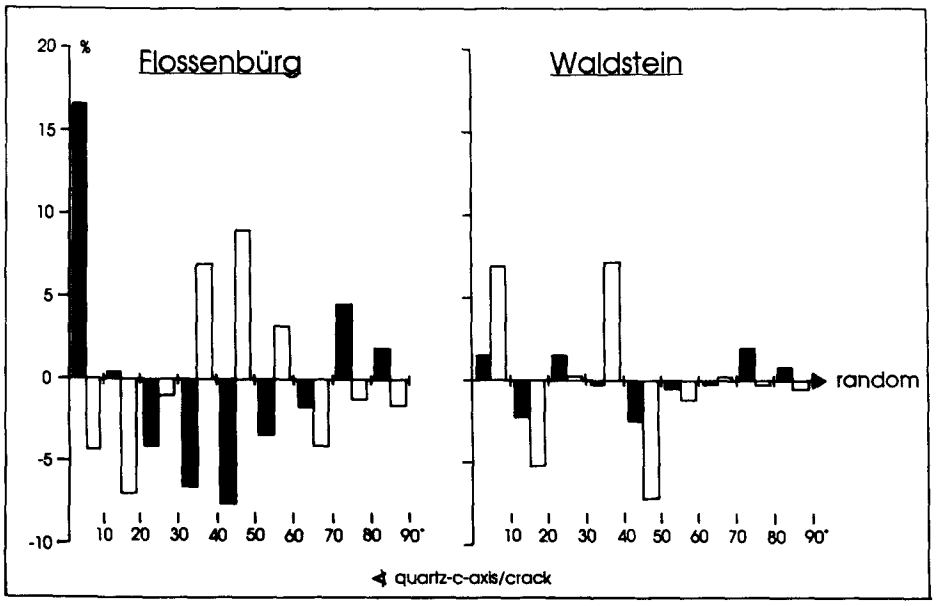

Fig. 5. Frequency plot of angles between cracks and quartz-*c*-axes of host grains; deviation in percentage from the theoretical frequency for random orientation of cracks as shown in Fig. 3. Open columns: open cracks; filled columns: healed cracks.

display weaker preferred orientations, especially in the Waldstein granite (Figs. 7g & h). In the Flossenbürg granite (Fig. 7g) steep open cracks mostly striking NW predominate. In addition, a weak pole maximum is developed which coincides with the maximum of the subhorizontal healed cracks. In the Waldstein granite (Fig. 7h) subhorizontal open cracks predominate while the pole maxima of steep open cracks scatter over a wide range.

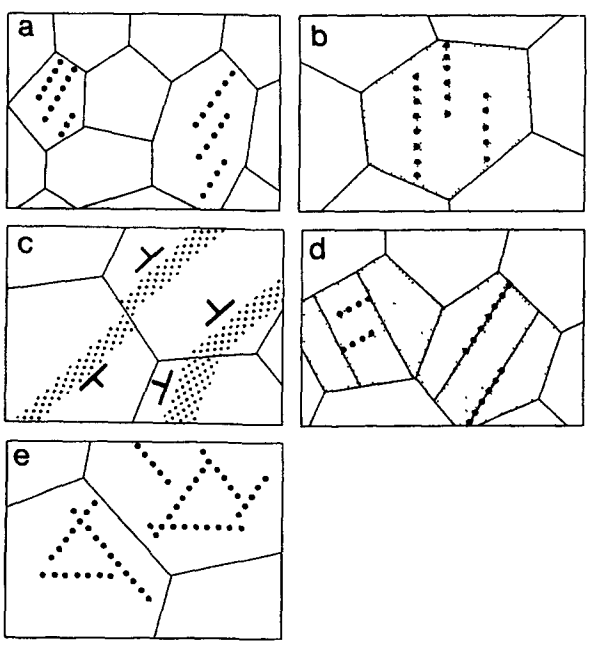

Fig. 6. Schematical illustration of microstructural features observed in the Waldstein and Flossenbürg granites suggesting that the direction of crack propagation is lattice-controlled. (a) Selective crack growth in grains with suitable lattice orientation with respect to the local stress directions. (b) Cracks parallel to polarization direction, shaded grain in extinction. (c) Change of strike and dip direction of cracks (dotted bands) when cutting interphase boundaries. (d) Symmetrical relationships to subgrain structures; shading marks areas of different extinction directions (deformation bands, subgrains). (e) Patterns with the symmetry of quartz.

Fluid inclusion data

With only a few exceptions, the secondary fluid inclusions within healed cracks consist of aqueous solutions of varying salinity and composition. For the discrimination of different crack generations and their relative age as well as for *P–T* estimates of crack healing the following general results (Fig. 8) are of special interest.

(1) Compared with the subhorizontal cracks the two sets of steep cracks show significant higher T_h values which also scatter over a larger range.

(2) For the Waldstein granite a differentiation between steep and subhorizontal cracks is also indicated by the salinities (lower T_m values for the subhorizontal set).

(3) According to their T_m and T_h characteristics, the two sets of steep cracks cannot be clearly separated, either in the Waldstein or in the Flossenbürg sample.

(4) As evident from observations on individual fluid inclusion trails, all three generations often exhibit a large scatter of the T_h values which together with the above mentioned microstructural criteria may point to repeated leakage during later reactivations.

The accurate determination of T_e values was limited by the small size of the inclusions (>10 μm) so that minute phase transitions from the frozen fluids could hardly be recognized. Thus, only few data are available which are insufficient for further discrimination of crack generations. The T_e values roughly vary between −10 and −35°C in the Waldstein samples and between −20 and −30°C in the Flossenbürg samples suggesting complex fluid systems probably dominated by NaCl (T_e = −20.8°C), KCl (T_e = −10.6°C) and $CaCl_2$ (T_e =

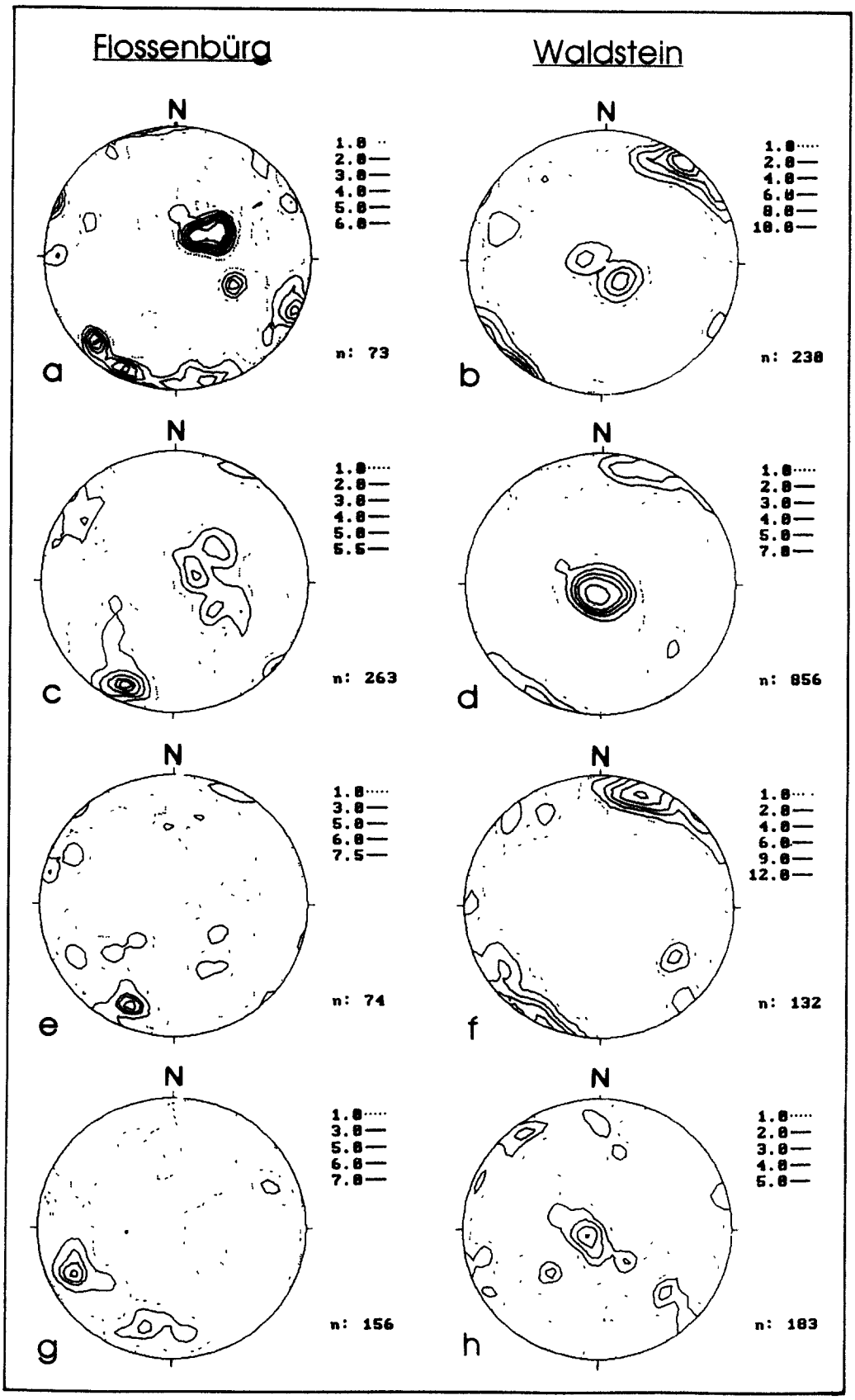

Fig 7. Pole figures for the Flossenburg and Waldstein granite, Schmidt net, lower hemisphere; contours in multiples of a random distribution (a) & (b) Macroscopic joints; (c) & (d) healed cracks; (e) short healed cracks (apparent crack length $< 150\,\mu m$); (f) subvertical healed cracks (apparent crack length $< 150\,\mu m$); (g) & (h) open cracks. For further explanation see text

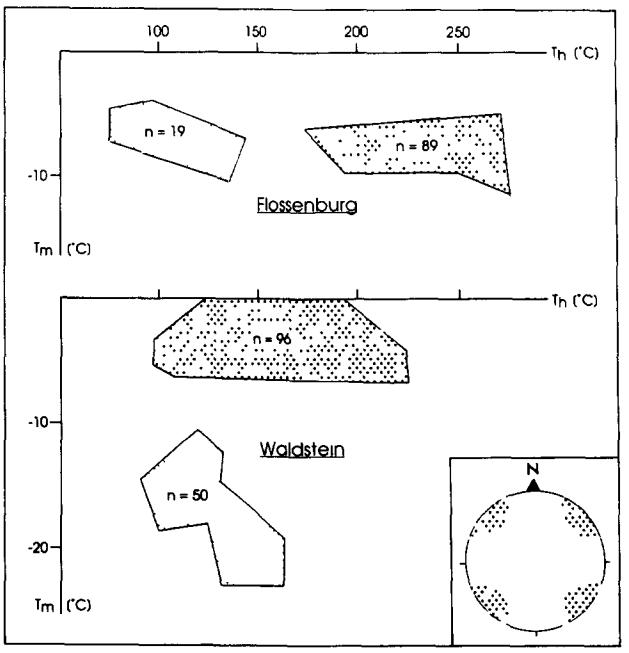

Fig. 8. Microthermometric data of secondary fluid inclusions in the Flossenburg and Waldstein granite (fields of most frequent T_m/T_h plots). Inset: schematical pole figure for related healed cracks; fields with heavy dots are plots for subvertical cracks; fields with light dots are plots for subhorizontal cracks

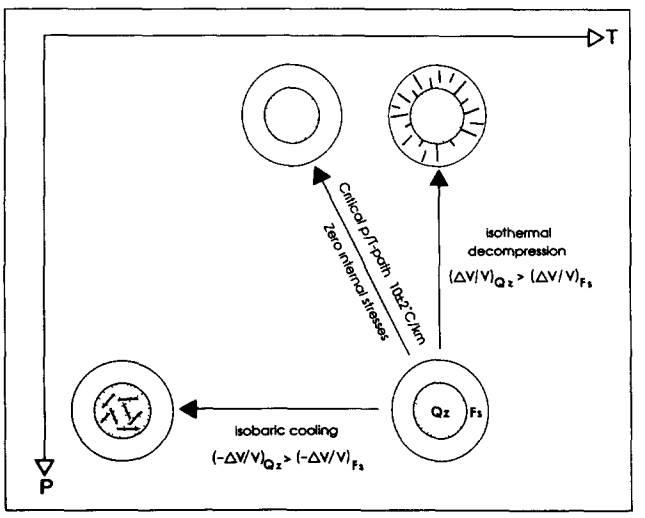

Fig. 9. Microcracking in quartz–feldspar rocks (bisphere) induced by internal stresses during cooling and decompression, for further explanation see text

−49.8°C) which are most common in aqueous crustal fluids (see references in Crawford 1981).

INTERPRETATION

Before discussing detailed models of microcracking in the granites during uplift which are in good agreement with the present data, the following basic interpretations should be emphasized.

(1) The congruence of the crack pole figures from both localities (at a distance of about 50 km, Fig. 1) agrees with the concept of relating preferred crack orientations to paleostress directions at the regional scale (e.g. Pecher *et al.* 1985, Kowallis *et al.* 1987). The regional significance is further confirmed by microcrack patterns observed in gneisses from KTB drill cores showing almost identical preferred orientations (Siegesmund *et al.* 1990).

(2) On the other hand, the higher crack densities in quartz as compared to adjacent feldspar grains may indicate that the initiation of microcracking is genetically related to internal stresses or differential volumetric strains at grain scale which especially holds for the healed cracks. However, there is no microstructural indication that microcracking was induced by residual stresses related to plastic deformation (no correlation between intensity of subgrain structures and crack densities).

(3) It can be concluded from many previous studies that the vast majority of microcracks in crystalline rocks are of the mode I type (e.g. Kranz 1983). Thus, for the determination of paleostress configurations it is reasonable to assume that the direction of the least normal stress (σ_3) was approximately parallel to the crack poles. Deflections from this orientation may occur due to the above described control by crystallographic directions and to stress heterogeneities at grain scale.

(4) For the healed cracks the fluid inclusion data suggest that the two steep sets have formed more or less simultaneously and at higher temperatures than the subhorizontal set; i.e. at an earlier stage of uplift (T_h values may be regarded as minimum temperatures of fluid trapping).

(5) The formation of the open cracks post-dates the healed cracks, and hence should be related to higher crustal levels.

Internal stresses as a cause of microcracking

During uplift of basement rocks, cooling and decompression generate internal stresses because of differential thermal contractions and compressibilities of the constituent minerals. These stresses may result in microcracking (Devore 1969, Savage 1978, Bruner 1984). According to their composition and fabric, granitic rocks may be described in simplified terms as a two component system (bisphere) consisting of a quartz core and a feldspar mantle (e.g. Nur & Simmons 1970). As compared to feldspars (and other rock forming minerals) quartz is characterized by significant higher values of compressibility (Birch 1966) and thermal expansion (Skinner 1966). Figure 9 schematically illustrates the initiation of microcracking within such a quartz–feldspar bisphere when subjected to changing temperatures or confining pressures. The two extreme P–T paths a granite may follow after crystallization are represented by isobaric cooling and isothermic decompression. It follows from the corresponding volumetric strains that the stronger elastic expansion of quartz during decompression favours microcracking in the feldspar mantle while the stronger thermal contraction of quartz during cooling leads to microcracking in the quartz core. According

to Bruner (1984) for granitic rocks a critical uplift path of approximately 10 ± 2° km^{-1} can be assumed along which a balance between thermal contraction and elastic expansion in the quartz–feldspar bisphere is approached so that internal stresses and related microcracking are minimized

In agreement with this model the concentration of healed cracks in quartz and their tendency to be oriented normal to the direction of maximum thermal expansion (Flossenburg sample, Fig. 5) suggest that the development of the healed cracks mainly resulted from cooling-induced thermal stresses at the grain scale (in the following referred to as 'thermal cracking'). The open cracks, however, are suggested to be induced mainly by tectonic (external) stresses because they are often transgranular, and probably initiated along rhombohedral cleavage planes in quartz.

Thermal cracking superposed by deviatoric external stresses

To explain the preferred orientation of the healed cracks at macroscopic or regional scale as well as the orthorhombic symmetry of crack patterns, the model of thermal cracking has to be extended by the superposition of an external deviatoric stress field (Fig. 10). This model suggests that a first generation of thermal cracks develops in the quartz core normal to the external σ_3 direction. This first set of cracks causes a local uncoupling of the quartz core from the σ_3 direction. Consequently, further thermal contraction of the now isolated quartz slices between cracks of the first set should produce a second set of cracks normal to σ_2. Due to subsequent crack healing this process may be polycyclic resulting in complex superpositions of orthorhombic crack patterns. Because of its deviating fluid inclusion characteristics (see Fig. 8) the third generation of healed cracks cannot be related to this first stage of thermal cracking but must have formed during later events (see below, model of successive microcracking).

This 'uncoupling model' offers a suitable explanation for the simultaneous development of two perpendicular sets of cracks without assuming a 90° reorientation of σ_3 to generate the second set, as has often been suggested in the literature (e.g. Plumb *et al.* 1984). Moreover, this model also provides the opportunity to determine all three principal normal stress directions (σ_1, σ_2, σ_3). However, the interpretation may be complicated by the above mentioned complex superposition of crack patterns making a clear identification of the two sets dubious

As mentioned above, these cracks show a preferred orientation both with respect to the quartz lattice as well as to the geographic directions. Thus, it is assumed that microcracking preferentially affected grains with a suitable lattice orientation with respect to the external deviatoric stress field. This is confirmed by the observed grain-related domains of varying crack densities (Fig. 6a).

There is no clear evidence that the open cracks developed as two related sets in the way, as was concluded for the healed cracks This may be further indication that the formation of the open cracks was largely controlled by external tectonic stresses

P–T *estimates*

For the healed cracks the *P–T* conditions of formation (fluid trapping) can be roughly estimated by intersecting the calculated isochores of the corresponding secondary fluid inclusions with appropriate palaeo-geothermal gradient (Fig. 11). According to numerous thermobarometric studies carried out in the Oberpfalz area during recent years (for compilation of data see Vollbrecht *et al.* 1990), for the now exposed basement level gradients between 40 and 60°C km^{-1} can be assumed during late-Variscan time. This leads to *P–T* ranges of about 1–3 kbar and 300–600°C for the two sets of steep cracks and 1–2 kbar and 150–350°C for the subhorizontal cracks, respectively. In contrast to the Waldstein granite the Flossenburg granite exhibits a distinct *P–T* gap between steep and horizontal cracks. One probable explanation is to relate this *P–T* gap to a phase of rapid uplift approaching the above mentioned critical path of minimized internal stresses (see Fig. 9). Accordingly, the formation of the open cracks should be restricted to higher crustal levels at *P–T* conditions roughly below 1 kbar and 150°C.

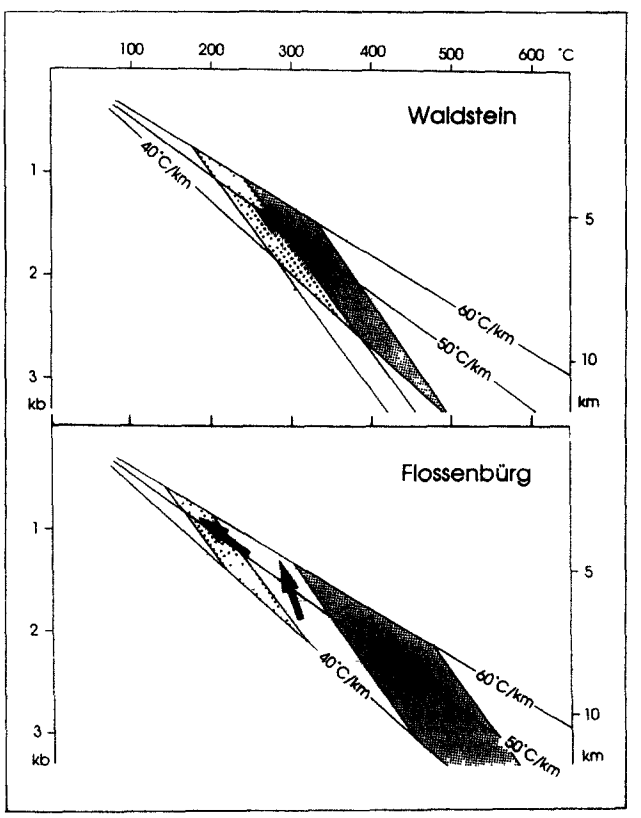

Fig 11 *P–T* estimates for healed microcracks in the Waldstein and Flossenburg granite; isochores after Crawford (1981); *P–T* fields are defined by intersecting the isochores with suitable geothermal gradients. Close dots are steep cracks, and spaced dots are subhorizontal cracks. For further explanation see text

Successive microcracking during uplift

On the basis of the present data from the Flossenbürg and Waldstein granite the following model of successive microcracking during cooling and uplift can be developed. The main steps are indicated by five generations of microcracks (here referred to as CI–CV; see Fig. 12).

The deep crustal levels ($P > 1$ kbar, $T > 150$°C) are characterized by the predominance of thermal cracking and subsequent crack healing. In the deepest level ($P \approx$ 1–3 kbar, σ_1 vertical) the development started with the simultaneous formation of two orthogonal sets of steep cracks (CI and CII). The inferred horizontal normal stress directions (σ_2 NE–SW, σ_3 NW–SE) correspond to the regional stress field during the late collision (indentation) stage as deduced from macroscopic structures (Weber 1986). At less depth ($P \approx$ 1–2 kbar, σ_2 vertical, σ_1 NE–SW) the CI cracks were reopened (leakage) and a new set of subhorizontal cracks was formed (CIII).

At high crustal levels ($P < 1$ kbar, $T < 150$°C) microcracking was mainly induced by (external) tectonic and gravitational stresses. So, in contrast to thermal cracking only one set of cracks developed normal to σ_3. Moreover, crack healing was inhibited probably due to low temperatures or lack of related fluids. At greater depths (σ_2 still assumed vertical) one set of steep NW–SE-striking cracks (CIV, Flossenbürg) formed indicating a NE–SW orientation of σ_3 which already corresponds roughly to the present *in situ* stress field in Middle Europe (e.g. see Kappelmeyer & Gerard 1989). At the same time the parallel CII cracks were reopened (leakage). Correspondingly, at the highest level (σ_3 vertical) subhorizontal open cracks (CV) formed and CIII cracks were reopened.

CONCLUSIONS

The results of our investigations suggest that uplift of granites may lead to successive microcracking of minerals under varying P–T conditions and changing stress field configurations resulting in complex superpositions of microcrack fabrics. The conclusions which seem to be of more than only local significance are as follows.

(1) At deep crustal levels intragranular microcracks are mainly induced by internal thermal stresses at the grain scale. In granites these stresses are caused by the strong thermal contraction of quartz with respect to the feldspar framework ('thermal cracking'). External deviatoric stresses may be low and only control the preferred direction of crack growth.

(2) The concept of thermal cracking implies that quartz-rich rocks represent zones of high crack concentration which may be responsible for geophysical discontinuities even at deeper crustal levels.

(3) Thermal cracking in granites may be largely suppressed during fast uplift along a critical path of about 10 ± 2°C km^{-1}. In this case the quartz–feldspar system

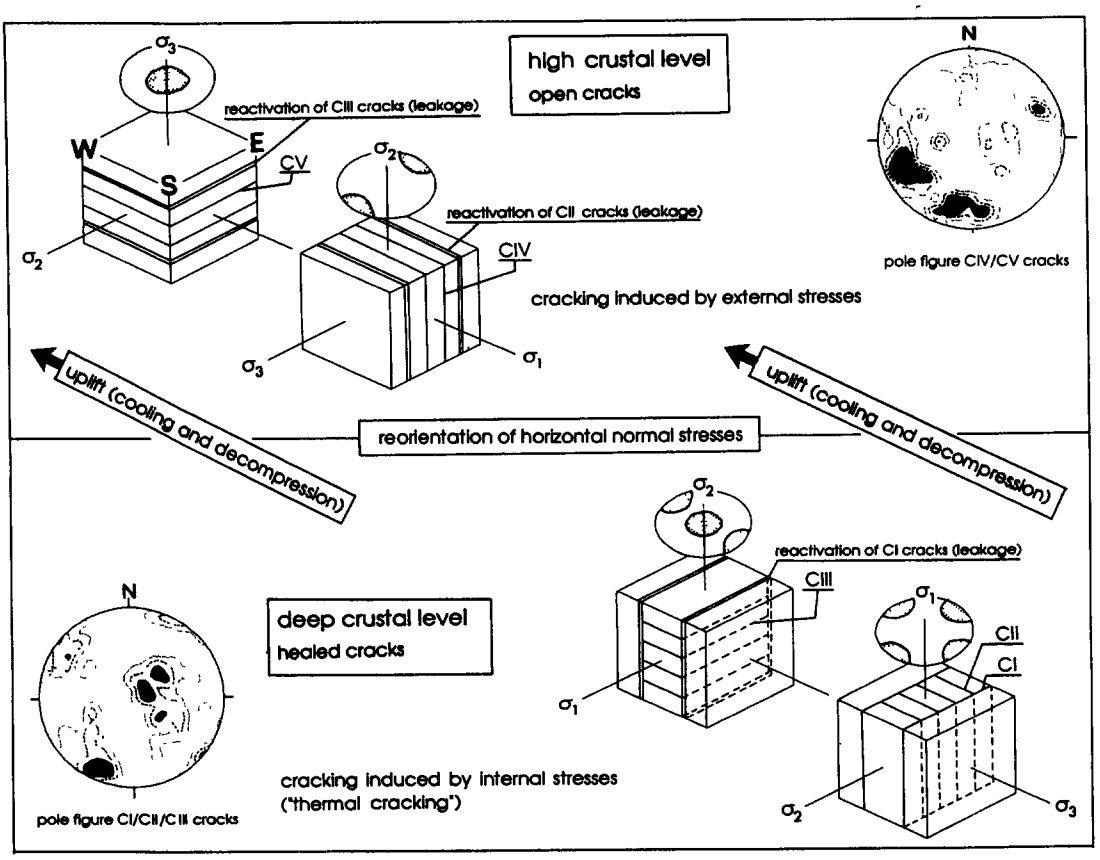

Fig. 12. Model of successive microcracking during uplift. Development is illustrated by four sample cubes with the crack generations CI–CV, the corresponding schematic pole figures and the inferred external stress directions. The geographic directions (W, S, E) are indicated at the corners of the uppermost cube. For further explanation see text.

approaches a balance between the volumetric strains due to thermal contraction and elastic expansion.

(4) Thermal cracking combined with local stress uncoupling at the grain scale leads to the simultaneous development of two orthogonal sets of cracks (normal to σ_3 and σ_2). Thus, microcracks of this type provide an opportunity of determining all three principal normal stress directions. On the other hand, this model questions the practice of relating paleostress directions to one set of cracks alone, a practice which requires a 90° switch of σ_3 in order to explain both sets of orthogonal crack patterns.

(5) The congruence of microcracks and joint patterns suggests that the formation of joints at shallow depths is influenced by pre-existing crack fabrics. Assuming a suitable configuration of the external stress field, the formation of macroscopic joints may be the result of further growth and step-wise joining of pre-existing cracks which represent loci of stress concentration.

Acknowledgements—This work was funded by the Deutsche Forschungsgemeinschaft (DFG) grant We 488/21-2,3. We wish to thank the colleagues of the KTB study group who provided helpful discussions. Special thanks are due to S. H. Treagus, W. M. Schwerdtner and two anonymous reviewers for their constructive comments which greatly improved the quality of this manuscript.

REFERENCES

Adam, J. F. 1989. Methoden und Algorithmen zur Verwaltung und Analyse axialer 3-D-Richtungsdaten und ihrer Belegungsdichten. *Gottinger Arb. Geol. Palaont.* **40**.

Behr, H. J. & Emmermann, R. 1987. Scientific objectives and site-selection studies of the Continental Deep Drilling Program of the Federal Republic of Germany (KTB). In: *Observation of the Continental Crust through Drilling II* (edited by Behr, H. J., Stehli, F. G. & Vidal, F.). Springer, Berlin, 85–119.

Bloss, F. D. 1957. Anisotropy of fracture in quartz. *Am. J. Sci.* **255**, 214–225.

Birch, F. 1966. Compressibility, elastic constants. In. *Handbook of Physical Constants* (rev. edn) (edited by Clark, S. P., Jr). *Mem. geol. Soc. Am.* **97**, 97–173.

Bruner, W. M. 1984. Crack growth during unroofing of crustal rocks: Effects on thermoelastic behaviour and near-surface stresses. *J. geophys. Res.* **89**, 4167–4184.

Cathelineau, M., Lespinasse, M., Bastoul, A. M., Bernard, C. & Leroy, J. 1990. Fluid migration during contact metamorphism: the use of oriented fluid inclusion trails for a time/space reconstruction. *Mineralog. Mag.* **54**, 169–182.

Crawford, M. L. 1981. Phase equilibria in aqueous fluid inclusions. In *Short Course in Fluid Inclusions: Applications to Petrology* (edited by Hollister, L. S. & Crawford, M. L.). Mineral. Assoc. Canada, 75–100.

DEKORP Research Group 1988. Results of the DEKORP 4/KTB Oberpfalz deep seismic reflection investigations. *J. Geophys.* **62**, 69–101.

Devore, G. W. 1969. Differential thermal contractions and compressibilities as a cause for mineral fracturing and annealing. *Contr. Geol.* **8**, 21–36.

Fischer, G. 1965. Uber die modale Zusammensetzung der Eruptiva im ostbayrischen Kristallin. *Geologica Bavarica* **55**, 7–33.

Franke, W. 1989. The Geological Framework of the KTB Drill Site, Oberpfalz. In: *The German Continental Deep Drilling Program (KTB)* (edited by Emmermann, R. & Wohlenberg, J.). Springer, Berlin, 37–54.

Fuchs, K. & Giese, P. 1987. Geophysical targets of the Continental Deep Drilling Program of the Federal Republic of Germany—Tomography of the crust and its permeability. A window into the lower crust and an *in-vivo* deep laboratory. In *Observation of the Continental Crust Through Drilling II* (edited by Behr, H. J., Stehli, F. G. & Vidal, F.). Springer, Berlin, 120–127.

Hansen, B. T., Teufel, S. & Ahrendt, H. 1989. Geochronology of the Moldanubian–Saxothuringian Transition Zone, Northeast Bavaria. In *The German Continental Deep Drilling Program (KTB)* (edited by Emmermann, R. & Wohlenberg, J.). Springer, Berlin, 55–65.

Hofmann, R. 1957. Kleintektonische Untersuchungen im Frankenwald, im Fichtelgebirge und in ihrem mesozoischen Vorland. *Z. dt. geol. Ges.* **109**, 340–360.

Jang, B.-A., Wang, H. F., Ren, X. & Kowallis, B. J. 1989. Precambrian paleostress from microcracks in the Wolf River batholith of central Wisconsin. *Bull. geol. Soc. Am.* **101**, 1457–1464.

Kappelmeyer, O. & Gerard, A. 1989. The European Geothermal Project at Soultz-Sous-Forets. In *Proc. Fourth Int. Sem. on the Results of EC Geothermal Energy Res. and Demonstration*, Florence, 27–30 April 1989 (edited by Louwrier, K., Staroste, E. & Garnish, J. D.). Kluwer Academic Publishers, Dordrecht.

Kern, H. & Wenk, H.-R. 1985. Anisotropy in rocks and the geological significance. In: *Preferred Orientation in Deformed Metals and Rocks: An Introduction to Modern Texture Analysis* (edited by Wenk, H.-R.). Academic Press, London, 537–555.

Kohler, H. & Muller-Sohnius, D. 1976. Erganzende Rb–Sr-Altersbestimmungen an Mineral- und Gesamtgesteinsproben des Leuchtenberger und des Flossenbürger Granits (NE-Bayern). *Neues Jb. Mineral. Mh.* **8**, 354–365.

Kohler, H., Müller-Sohnius, D. & Camman, K. 1974. Rb–Sr Altersbestimmungen an Mineral- und Gesamtgesteinsproben des Leuchtenberger und Flossenburger Granits, NE Bayern. *Neues Jb. Mineral. Abh.* **123**, 63–85.

Kossmat, F. 1927. Zur Gliederung des varistischen Gebirgsbaues. *Abh. sachs. geol. Landesamts* **1**.

Kowallis, B. J., Wang, H. F. & Jang, B.-A. 1987. Healed microcrack orientations in granite from Illinois borehole UPH-3 and their relationship to the rock's stress history. *Tectonophysics* **135**, 297–306.

Kranz, R. L. 1983. Microcracks in rocks: a review. *Tectonophysics* **100**, 449–480.

Kreuzer, H., Seidel, E., Schussler, U., Okrusch, M., Lenz, K.-L. & Raschka, H. 1989. K–Ar geochronology of different tectonic units at the northwestern margin of the Bohemian Massif. *Tectonophysics* **157**, 149–178.

Nover, G., Buntebarth, G., Kern, H., Pohl, I., Pusch, G., Schopper, J. R., Schult, A. & Will, G. 1989. Petrophysical investigations on core samples of the KTB. *Scientific Drilling* **1**, 135–142.

Nur, A. & Simmons, G. 1970. The origin of small cracks in igneous rocks. *Int. J. Rock Mech. & Mining Sci.* **7**, 307–314.

Pecher, A., Lespinasse, M. & Leroy, J. 1985. Relations between inclusion trails and regional stress field: a tool for fluid chronology—An example of an intragranitic uranium ore deposit (northwest Massif Central, France). *Lithos* **18**, 229–237.

Peng, S. S. & Johnson, A. M. 1972. Crack growth and faulting in cylindrical specimens of Chelmsford granite. *Int. J. Rock Mech. & Mining Sci.* **9**, 37–86.

Plumb, R., Engelder, T. & Yale, D. 1984. Near-surface *in situ* stress 3. Correlation with microcrack fabric within the New Hampshire granites. *J. geophys. Res.* **89**, 9350–9364.

Poty, B., Leroy, J. & Jachimowicz, L. 1976. Un nouvel appareil pour la measure des temperatures sous le microscope: L'installation de microthermometrie Chaixmeca. *Bull. Soc. fr. Minér. Cristallogr.* **99**, 182–186.

Richter, P. & Stettner, G. 1979. Geochemische und petrographische Untersuchungen der Fichtelgebirgsgranite. *Geologica Bavarica* **78**, 1–129.

Roedder, E. 1984. *Fluid Inclusions. Reviews in Mineralogy* **12** (edited by Ribbe, P. H.). Mineralogical Society of America.

Savage, W. Z. 1978. The development of residual stress in cooling rock bodies. *Geophys. Res. Lett.* **5**, 633–636.

Schreyer, W. 1966. Metamorpher Ubergang Moldanubikum/Saxothuringikum ostlich Tirschenreuth/Opf., nachgewiesen durch phasenpetrologische Analyse. *Geol. Rdsch.* **55**, 491–509.

Schussler, U., Oppermann, U., Kreuzer, H., Seidel, E., Okrusch, M., Lenz, K.-L. & Raschka, H. 1986. Zur Altersstellung des ostbayrischen Kristallins: Ergebnisse neuer K–Ar-Datierungen. *Geologica Bavarica* **89**, 21–47.

Shepherd, T. J., Rankin, A. H. & Alderton, D. H. M. 1985. *A Practical Guide to Fluid Inclusion Studies*. Blackie & Sons, Glasgow.

Siddans, A. W. B. 1976. Deformed rocks and their textures. *Phil. Trans. R. Soc. Lond.* **A283**, 43–54.

Siegesmund, S , Kern, H. & Vollbrecht, A. 1991. The effect of oriented intragranular and grain boundary cracks on seismic velocities in an ultramylonite. *Tectonophysics* **186**, 241–251

Siegesmund, S , Vollbrecht, A. & Weber, K. 1990 Gefugekundliche Untersuchungen im KTB. *Die Geowissenschaften* **8**, 287–294.

Skinner, B. J. 1966. Thermal expansion. In: *Handbook of Physical Constants* (rev. edn) (edited by Clark, S. P , Jr). *Mem. geol. Soc. Am.* **97**, 75–96

Stein, E. 1988 Die strukturgeologische Entwicklung im Ubergangsbereich Saxothuringikum/Moldanubikum in NE-Bayern. *Geologica Bavarica* **92**, 5–131.

Teufel, S. 1988. Vergleichende U–Pb- und Rb–Sr-Altersbestimmungen an Gesteinen des Ubergangsbereiches Saxothuringikum/Moldanubikum, NE-Bayern. *Göttinger Arb. Geol. Paläont.* **35**.

Thill, R. E., Willard, R. J. & Bur, T. R. 1969 Correlation of longitudinal velocity variation with rock fabrics. *J. geophys. Res.* **74**, 4897–4909.

Vollbrecht, A., Heidelbach, F. & Weber, K. 1990. Mikrorisse in Gneisen der ZEV (KTB-Vorbohrung, Bohrung Püllersreuth). *KTB-Report* 90-4, 514.

Vollbrecht, A., Weber, K & Schmoll, J 1989 Structural model for the Saxothuringian–Moldanubian suture in the Variscan basement of the Oberpfalz (Northeastern Bavaria, F.R.G.) interpreted from geophysical data. *Tectonophysics* **157**, 123–133.

Wagener-Lohse, C. & Blümel, P. 1984. Prograde Metamorphose vom Niederdruck-Typ in der Grenzzone Saxothuringikum/Moldanubikum E'Tirschenreuth. *Fortschr. Miner. Beih.* **62**, 254–255

Weber, K. & Vollbrecht, A. 1989. The crustal structure at the KTB Drill Site, Oberpfalz. In: *The German Continental Deep Drilling Program (KTB)* (edited by Emmermann, R. & Wohlenberg, J). Springer, Berlin.

Weber, K. 1986. The mid-European Variscides in terms of allochthonous terranes. In: *Proc. Third Workshop on the European Geotraverse (EGT) Project: The Central Segment*, 14–16 April 1986 (edited by Freeman, R., Mueller, St. & Giese, P.). Bad Honnef, 73–81.

Wendt, J., Kreuzer, H., Muller, P. und Schmid, H. 1986. Gesamtgesteins- und Mineraldatierungen des Falkenberger Granits. *Geol. Jb.* **E34**, 5–66.

Ziegler, P. A. 1984. Caledonian and crustal consolidation of Western and Central Europe—a working hypothesis. *Geologie Mijnb.* **63**, 93–108.